JOC The Journal of Organic Chemistry

Article

pubs.acs.org/joc

Metal-assisted Lossen Rearrangement

Lucie Jašíková, Eva Hanikýřová, Anton Škríba, Juraj Jašík, and Jana Roithová*

Department of Organic Chemistry, Faculty of Science, Charles University in Prague, Hlavova 2030/8, 12843 Prague 2, Czech Republic

Supporting Information

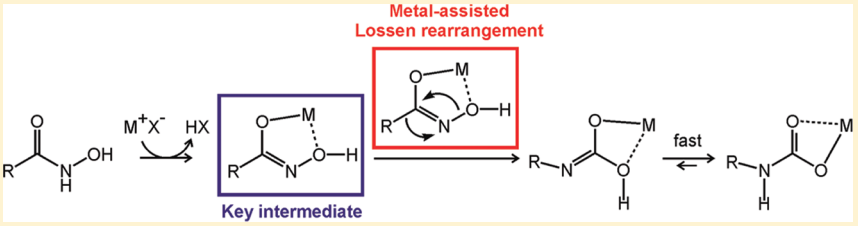

ABSTRACT: A new reaction mechanism for the Lossen rearrangement of hydroxamic acids catalyzed by basic salts is presented. It is shown that the rearrangement proceeds in metal complexes of deprotonated hydroxamic acids. The deprotonation can occur either at the oxygen atom (observed for the zinc complexes) or at the nitrogen atom (observed for the potassium complexes). Both anionic forms are characterized by infrared multiphoton dissociation spectroscopy. The rearrangements proceed from the reactive *N*-deprotonated metal hydroxamates and lead to metal carbamates. The mechanism is elucidated by computational chemistry, mass-spectrometric studies, and preparative experiments.

INTRODUCTION

The Lossen rearrangement is one of three text-book rearrangements (together with the Curtius and Hofmann rearrangements) in which derivatives of carboxylic acids (hydroxamic acids, azides, and amides, respectively) are transformed via transient acyl nitrenes to isocyanate intermediates. Isocyanate intermediates can be either trapped by a nucleophile to form derivatives of the corresponding carbamic acids or degraded to the respective amines in the presence of water (Scheme 1). The classical Lossen rearrangement starts with the formation of a mixed anhydride from a hydroxamic acid and another acid derivative such as acetanhydride or tosyl chloride.[1,2] Heating with a base then leads to the elimination of acetate or tosylate, respectively, concomitant with the rearrangement to an isocyanate.

The mixed anhydride has to be either prepared in a separate step or it can be generated in situ. The latter procedure has the disadvantage that the formed isocyanate can react with free hydroxamic acid to yield the corresponding *O*-carbamoylhydroxamate, which under the heating affords a symmetrically substituted derivative of urea.[3,4] Alternative procedures for the Lossen rearrangement avoiding this undesired self-dimerization are based on reactions of hydroxamic acids with dehydrating agents such as dicyclohexylcarbodiimide (DCC)[5,6] or carbonyldiimidazole (DCI).[7]

The simplest approach has been shown recently: The rearrangement of aromatic hydroxamic acids can be easily achieved by heating with a base such as K_2CO_3.[8] The reaction mechanism suggested for the base-catalyzed reaction (Scheme 2) is based on the analogy with the original mechanism depicted in Scheme 1. Thus, a mixed anhydride of hydroxamic and carbamic acids, *O*-carbamoylhydroxamate, is suggested as a key intermediate, which decomposes to yield the corresponding amine, CO_2, and isocyanate. The isocyanate returns to the catalytic cycle and reacts with the hydroxamic acid to afford another molecule of *O*-carbamoylhydroxamate. There are, however, many open questions. Thus, why should the *O*-carbamoylhydroxamate intermediate decompose to yield the corresponding amine in the base-catalyzed reaction, while the decomposition of the isolated *O*-carbamoylhydroxamate leads to the formation of the urea product? Is this change in reactivity an effect of the solvent? Are there some specific effects of the bases, or is the reaction just dependent on the pK_b of a particular base? In this paper, we present an alternative mechanism, which is not based on the formation of *O*-carbamoylhydroxamate, but instead the reaction proceeds under catalysis of metal ions, which are present in the solution as counterions of the added base.

RESULTS AND DISCUSSION

We have recently studied the complexation abilities of hydroxamic acids in the gas phase.[9] In particular, we have addressed the competitive complexation of zinc ions by acetate and acetohydroxamate. It has been shown that, upon the collisional activation, acetohydroxamate coordinated to zinc(II) loses a neutral isocyanate. This finding has inspired us to investigate a possible correlation between this gas-phase rearrangement and the mechanism operating in the condensed phase during the Lossen rearrangements catalyzed by basic metal salts.

Received: January 10, 2012
Published: February 23, 2012

   dx.doi.org/10.1021/jo300031f | *J. Org. Chem.* 2012, 77, 2829–2836

Scheme 1. Mechanism of the Classical Lossen Rearrangement

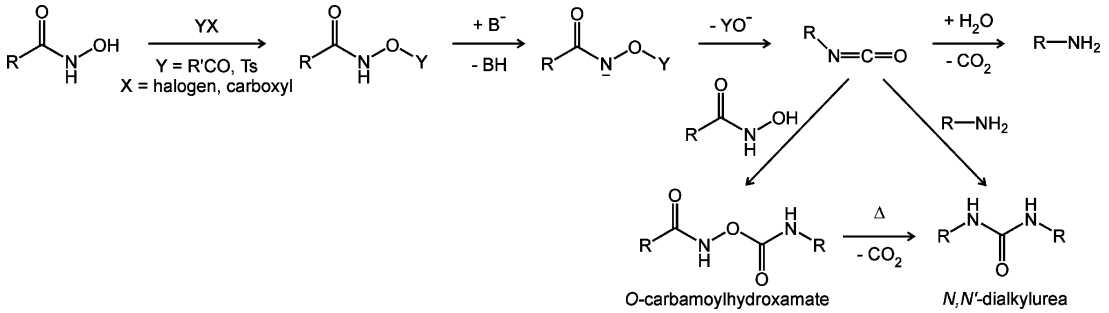

Scheme 2. Suggested Mechanism of the Base-catalyzed Lossen Rearrangement

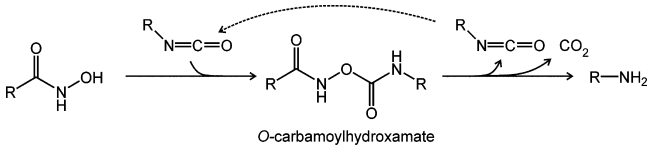

The reaction is induced by deprotonation of the nitrogen atom of the hydroxamic acid in most of the designed procedures (see Scheme 1). For free hydroxamic acids, the site of the deprotonation has been a subject of controversy.[10] There exists evidence for preferred *N*-deprotonation, but under certain conditions and for some hydroxamic acids also *O*-deprotonation can prevail. However, in the presence of a metal cation there exist numerous experimental evidence (crystal structures) that the hydroxamate is coordinated in the *O*-deprotonated form.[11]

Accordingly, let us first consider the structure of metal hydroxamate ions in the gas phase. Structures of ionic metal complexes in the gas phase can be elucidated by infrared multiphoton dissociation (IRMPD) spectroscopy.[12] This method is based on the investigation of fragmentations induced by the absorption of IR photons. It is a multiphoton method, because the absorption of several IR photons is necessary for the cleavage of (usually covalent) bonds. The IR absorption is resonantly enhanced at the position of an absorption band of the investigated ions, which consequently leads to a more abundant fragmentation. The dependence of the fragmentation yield on the wavelength of the IR photons hence provides an experimental (multiphoton) IR spectrum of gaseous ions.

First, we have spectroscopically investigated complex of zinc with the benzhydroxamate counterion $(\mathbf{1}\text{-H})^-$. Zinc ions in the gas phase are preferentially tetracoordinated;[13] therefore, we cannot generate the bare $[Zn(\mathbf{1}\text{-H})]^+$ cations, but instead a complex $[Zn(\mathbf{1}\text{-H})(\mathbf{1})]^+$ is formed. The IRMPD spectrum of this complex is dominated by two bands at 1520 and 1650 cm^{-1} (see the SI). On the basis of comparison with the theoretical spectra, these bands are assigned to the carbonyl vibration of the *O*-deprotonated and neutral hydroxamic acid, respectively. The theoretical spectra of $[Zn(\mathbf{1}\text{-H})(\mathbf{1})]^+$ contain overlapping bands corresponding to the deprotonated and to the neutral hydroxamic acid and therefore the interpretation is not straightforward (for details see the SI). We have therefore rather decided to replace the neutral hydroxamic acid by phenanthroline ligand (Phen).

Figure 1 shows the IRMPD spectrum of $[Zn(\mathbf{1}\text{-H})(Phen)]^+$. The irradiation (or collisional activation, see lower) induces exclusively elimination of phenylisocyanate (PhNCO), which

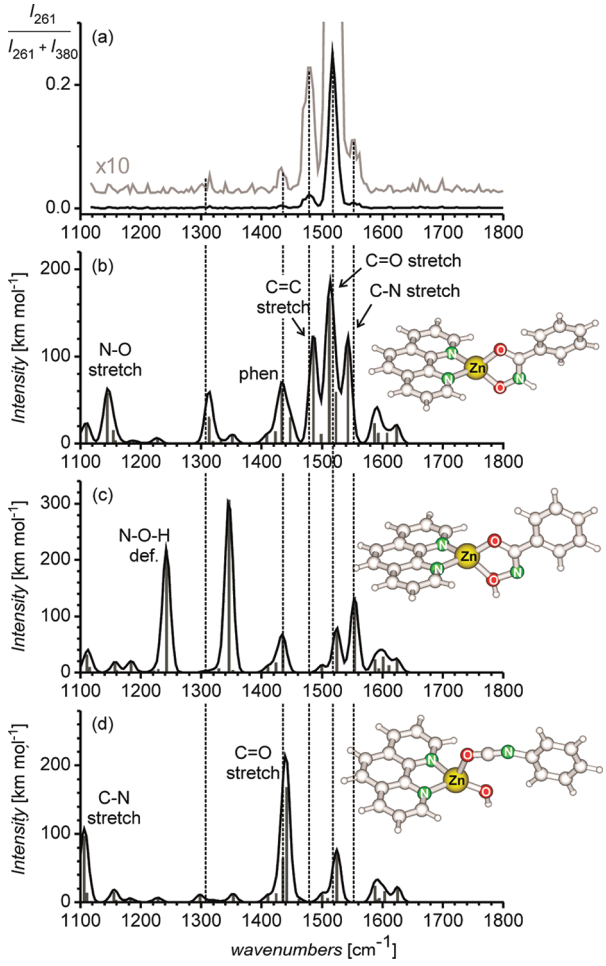

Figure 1. IRMPD spectrum of $[Zn(\mathbf{1}\text{-H})(Phen)]^+$ (a) and its comparison with theoretically calculated IR spectra of different isomers of the complex (b–d). The theoretical spectra are shown as gray bars, the black solid lines show the theoretical spectra folded with a Gaussian function (fwhm = 16 cm^{-1}). Notations I_{380} and I_{261} refer to the relative intensities of the parent complex $[Zn(\mathbf{1}\text{-H})(Phen)]^+$ (m/z 380) and the fragment $[Zn(OH)(Phen)]^+$ (m/z 261), respectively.

thus corresponds to the occurrence of the Lossen rearrangement. The corresponding IRMPD spectrum shows three main peaks at about 1480, 1520, and 1550 cm^{-1}. Detailed inspection reveals also two minor features at 1430 and 1310 cm^{-1}. To interpret the spectrum, we have explored possible structures of the complex by DFT calculations.

The most stable isomer of the $[Zn(\mathbf{1}\text{-H})(Phen)]^+$ complex bears benzhydroxamic acid deprotonated at the oxygen atom (A1_Zn, Figure 1b). The corresponding theoretical IR

dx.doi.org/10.1021/jo300031f | J. Org. Chem. 2012, 77, 2829–2836

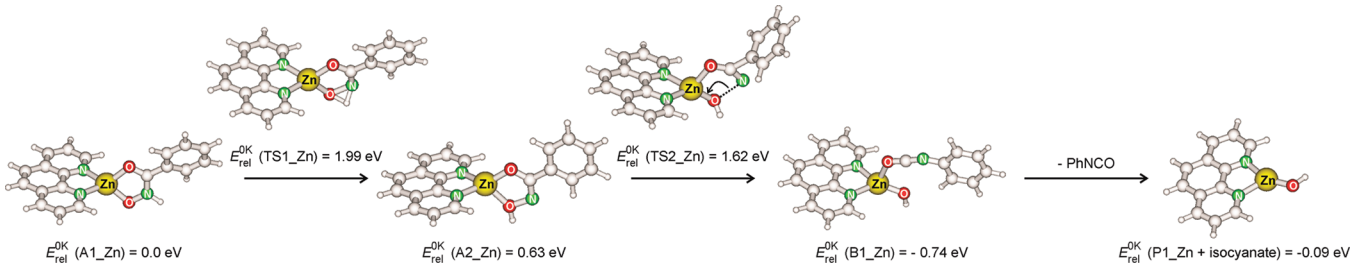

Figure 2. B3LYP/TZVP potential-energy surface for the Lossen rearrangement of within the $[Zn(\mathbf{1}\text{-H})(Phen)]^+$ complex. The energies are given at 0 K relative to E^{0K}(A1_Zn) = −2826.524477 hartree.

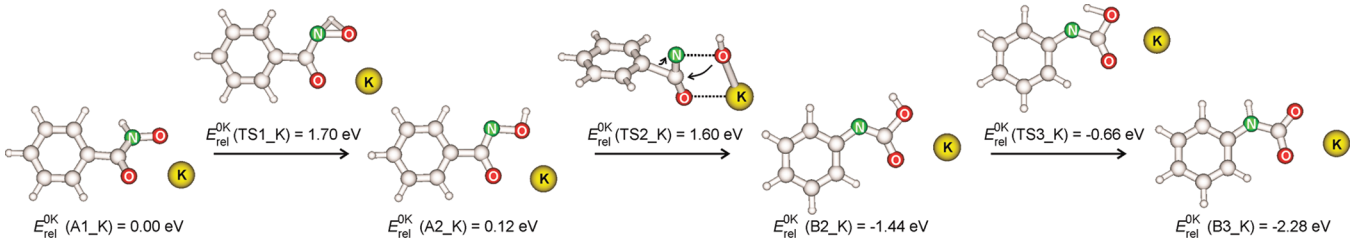

Figure 3. B3LYP/TZVP potential-energy surface for the potassium-assisted Lossen rearrangement. Energies refer to 0 K in the gas phase and are given relative to E^{0K}(A1_K) = −1075.552235 hartree; energies in DMF at 298 K can be found in Table 2.

spectrum agrees well with the IRMPD spectrum. The major peak at 1520 cm^{-1} corresponds to the CO stretch of the carbonyl group (as also found above for $[Zn(\mathbf{1}\text{-H})(\mathbf{1})]^+$). The peak at 1480 cm^{-1} originates from the C═C stretches of the phenyl ring, and the peak at 1550 cm^{-1} corresponds to the C−N stretch of the hydroxamate group. The minor peaks come from the vibrations of the phenanthroline ring (1430 cm^{-1}) and benzhydroxamate (1310 cm^{-1}).

The alternative isomer with the hydroxamate deprotonated at the nitrogen atom (A2_Zn) lies 0.63 eV higher in energy than the most stable isomer. In accordance, the IR spectrum (Figure 1c) does not agree with the experimental IRMPD features of the $[Zn(\mathbf{1}\text{-H})(Phen)]^+$ complex. We have also considered that we could detect fragmentation of the complex, which had already undergone the Lossen rearrangement. In such a case, the zinc cation would be coordinated by phenanthroline, phenylisocyanate, and a hydroxo ligand (B1_Zn). The rearrangement is exothermic and this complex lies 0.74 eV below the energy of the most stable isomer of zinc benzhydroxamate (cf. Figure 2). However, the computed spectrum of this complex (Figure 1d) does not agree with the experimental IRMPD spectrum of $[Zn(\mathbf{1}\text{-H})(Phen)]^+$. We can hence conclude that we transfer the most stable isomer of the complex between phenanthroline and zinc benzhydroxamate to the gas phase and by irradiation with IR photons we promote the Lossen rearrangement and the concomitant loss of phenylisocyanate.

The computed potential-energy surface for this rearrangement (Figure 2) reveals that the rate-determining step corresponds to the migration of the hydrogen atom from the nitrogen atom to the oxygen atom of benzhydroxamate. The corresponding transition structure (TS1_Zn) lies 1.99 eV higher in energy than the initial isomer A1_Zn. The subsequent rearrangement consists in the cleavage of the N−O bond associated with the migration of the phenyl group to the nitrogen atom and leads to the product ion B1_Zn. This step proceeds via an energy barrier of 0.99 eV (TS2; 1.62 eV above the energy of A1_Zn) and it is highly exothermic. We have also searched for a nitrene intermediate,[14] but it is not a minimum at the level of theory chosen. The product complex finally decomposes by the loss of phenylisocyanate, which still results in exothermicity of 0.09 eV for the whole fragmentation pathway.

We have determined the activation energy for the rearrangement in the gas phase by energy-resolved collision induced dissociation experiment (experimental details and data can be found in the SI).[15,16] Fragmentation of the $[Zn(\mathbf{1}\text{-H})(Phen)]^+$ complex leads exclusively to the loss of phenylisocyanate. Analysis of the relative cross section for this fragmentation leads to a threshold energy of 1.8 ± 0.2 eV, which compares reasonably well to the theoretically predicted activation energy of 1.99 eV. The associated transition structure corresponds to the hydrogen-atom migration from the nitrogen atom to the oxygen atom and the barrier can be lowered by tunneling.[17] More probably, however, the experimental threshold is slightly underestimated, because the studied ions are not thermalized. We have typically encountered underestimations of threshold energies by up to 0.2 eV, which perfectly fits the results here.[18]

We note in passing that we have tried to trap the possible nitrene intermediate experimentally. To this end, the mass-selected ions were collided at various collision energies (ranging from 0 to 5 eV in the center-of-mass framework) with cyclooctene. Cyclooctene was chosen because it is a very reactive alkene and hence we expected that the nitrene intermediate could undergo an addition reaction to the double bond of cyclooctene. Despite large efforts, we have never detected any trace of the addition product. This may serve as an indirect hint that the nitrene is not formed during the rearrangements and that the reaction proceeds in a single step as indeed suggested by the DFT calculations.

In summary, we so far have shown that the Lossen rearrangement proceeds in the zinc complexes in the gas phase. Next, the relevance for the base-catalyzed reaction in the condensed phase will be addressed. Hoshino et al. showed that the most efficient base is potassium carbonate.[8] We have therefore performed further calculations and experiments for potassium complexes.

dx.doi.org/10.1021/jo300031f | J. Org. Chem. 2012, 77, 2829−2836

The theoretical calculations show that the potential-energy surface of the rearrangement of the potassium salt is slightly different from that found for the zinc complex (Figure 3). The most stable complex again corresponds to the coordination of potassium to the benzhydroxamic acid deprotonated at the oxygen atom (A1_K). However, the alternative isomer deprotonated at the nitrogen atom (A2_K) is much closer in energy and it lies only 0.12 eV above A1_K. The hydrogen rearrangement proceeds via an energy barrier (TS1_K) of 1.70 eV. While the transition structure for the subsequent Lossen rearrangement is very similar to that found above for the zinc complex, the reaction sequence does not lead to the formation of potassium hydroxide with coordinated phenylisocyanate, but the hydroxyl group rather adds to the carbon atom of phenylisocyanate and forms *N*-phenylcarbamate deprotonated at the nitrogen atom (B2_K). The transition structure for the Lossen rearrangement (TS2_K) lies 1.60 eV above the energy of A1_K and the reaction sequence is 1.44 eV exothermic. The more stable isomer of potassium *N*-phenylcarbamate deprotonated at the oxygen atom (B3_K) is formed via an energy barrier (TS3_K), which is substantially lower than those in both preceding steps. Hence, this step is not expected to play a role in the kinetics of the reaction. The overall reaction is highly exothermic in that potassium *N*-phenylcarbamate is 2.28 eV more stable than potassium benzhydroxamate.

In the original paper of Hoshino et al. on the base-mediated Lossen rearrangement,[8] it has been reported that the yield of the amine formed by the Lossen rearrangement exceeds 90% if K_2CO_3 is used as the catalyst (2 h in DMF at 90 °C). If Na_2CO_3 or Li_2CO_3 are used as catalysts under the same conditions, the yields drop to 81% and 12%, respectively. Hence, we have performed analogous potential-energy surface calculations with sodium and lithium cations in order to check, whether the suggested mechanism accounts for these experimental results (Table 1). The activation energies for the initial hydrogen migration slightly rise in the order K < Na < Li, which is reflected also in increasing relative energies of the *N*-deprotonated forms of the complex. The relative energy of the transition structure for the subsequent Lossen rearrangement is about the same for all complexes, which means that with respect to the energy of the reactive *N*-deprotonated form, the energy barrier decreases from the potassium complex (1.48 eV) to the sodium complex (1.44 eV) and is smallest for the lithium complex (1.37).

Table 1. Energetics of the Metal-assisted Lossen Rearrangement in the Gas Phase Catalyzed by Potassium, Sodium, Lithium, and Zinc[a]

	A1_M	TS1_M	A2_M	TS2_M	B2_M
[(**1**-H)K]	0.00	1.70	0.12	1.60	−1.44
[(**1**-H)K(DMF)$_2$]	0.00	1.69	0.03	1.58	−1.40
[(**1**-H)Na]	0.00	1.73	0.18	1.62	−1.01
[(**1**-H)Li]	0.00	1.77	0.22	1.59	−0.77
[(**2**-H)K]$^+$	0.15	1.83	0.00	1.97	−1.79
[(**1**-H)Zn]$^+$	0.00	2.13	0.86	1.21	−1.75[b]
[(**1**-H)Zn(Phen)]$^+$	0.00	1.99	0.63	1.62	−0.74[b]
[(**1**-H)Zn(DMF)$_2$]$^+$	0.00	1.96	0.59	1.56	−0.75[b]
(**1**-H)$^-$	0.27	1.79	0.00	1.87	−2.16

[a]Relative energies are given at 0 K in eV. [b]Product corresponds to B1_Zn isomer with separated isocyanate and hydroxo ligands coordinated to the zinc cation.

The reaction could alternatively proceed without the involvement of a metal and hence for the bare anion generated from hydroxamic acid upon interaction with a base. The *N*-deprotonated forms of free hydroxamates are preferred. For the benzhydroxamate, the *N*-deprotonated anion is 0.27 eV more stable than the *O*-deprotonated anion. The barrier for the Lossen rearrangement amounts to 1.87 eV. Hence, the reaction can proceed also for a free hydroxamate, but the complexation with a metal decreases the energy barrier for the rearrangement and thus catalyzes the reaction.

In the condensed phase, the height of the first energy barrier can be significantly decreased in the presence of proton shuttles such water or other protic molecules.[19] The second energy barrier corresponding to the actual Lossen rearrangement is very similar for all reactant complexes. Therefore, it is most likely that the equilibrium between the isomers A1_M and A2_M or a direct preferential formation of A2_M is decisive for the overall efficiency of the reaction.[20]

The relative stabilities of A1_M and A2_M can be influenced by solvent. The reactions were performed in DMF (*N*,*N*-dimethylformamide), which we have here accounted for by PCM (polarized continuum model) calculations of the solvent effect of DMF (Table 2). It can be seen that the solvent significantly stabilizes the *N*-deprotonated complex (A2_M, cf. Tables 1 and 2) with respect to the *O*-deprotonated complex. For the potassium complexes (and also for the sodium complexes if we consider the Gibbs energies at 298 K—values in parentheses in Table 2), the reactive *N*-deprotonated complex becomes the energetically favored one. The energy barriers associated with the Lossen rearrangement are very similar for all studied complexes. We have also computationally explored effects of other solvents. The relative energies are, however, almost the same for all studied solvents (*N*,*N*′-dimethylformamide, dimethylsulfoxide, water, and ethanol); details can be found in the SI. For the free anions in DMF, the *N*-deprotonated hydroxamate is even more energetically preferred to the *O*-deprotonated anion than in the gas phase. The barrier for the rearrangements, however, stays on the order of 1.88 eV, which is about 0.3 eV higher than for the metal complexes.

For all metals investigated here, the reactive form of the complex with *N*-deprotonated hydroxamate is most energetically disfavored for zinc. We have probed the zinc complexes also by the calculations in DMF. For the simplest model complex [(**1**-H)Zn]$^+$, a large energetic disfavor for the reactive *N*-deprotonated isomer (E_{rel} = 0.86 eV) has been found in the gas phase (Table 1), which is most probably due to the coordinative unsaturation of the zinc ion. If we consider energies of the complex [(**1**-H)Zn(DMF)$_2$]$^+$ with two coordinated molecules of DMF, then the energy difference between the *O*- and *N*-deprotonated complexes drops to 0.59 eV. Consideration of the solvent effect leads to the value of 0.37 eV, which nevertheless is still considerably higher than found for the alkali metals.

We note in passing that the effect of the number of the coordinated ligands is much smaller for the potassium complexes than for the zinc complexes. Relative energies along the potential-energy surface for the rearrangements within the [(**1**-H)K(DMF)$_2$] complex, where two molecules of DMF are coordinated to the potassium cation, are very similar to those for the [(**1**-H)K] complex (cf. the first two entries in Table 1). The biggest effect is found for the relative stability of

dx.doi.org/10.1021/jo300031f | J. Org. Chem. 2012, 77, 2829−2836

Table 2. Energetics of the Metal-assisted Lossen Rearrangement in DMF Catalyzed by Potassium, Sodium, Lithium, and Zinc[a,b]

	A1_M	TS1_M	A2_M	TS2_M	B2_M
[(**1**-H)K]	0.03 (0.05)	1.73 (1.74)	0.00 (0.00)	1.59 (1.55)	−1.72 (−1.76)
[(**1**-H)Na]	0.00 (0.02)	1.73 (1.79)	0.01 (0.00)	1.59 (1.57)	−1.47 (−1.48)
[(**1**-H)Li]	0.00 (0.00)	1.76 (1.75)	0.06 (0.04)	1.62 (1.58)	−1.34 (−1.36)
$[(\mathbf{1}\text{-H})Zn]^+$	0.00 (0.00)	1.97 (1.97)	0.46 (0.45)	1.55 (1.52)	−0.95 (−1.04)
$[(\mathbf{1}\text{-H})Zn(DMF)_2]^+$	0.00 (0.00)	1.93 (1.88)	0.37 (0.34)	1.58 (1.54)	−0.76 (−0.90)
$(\mathbf{1}\text{-H})^-$	0.32 (0.35)	1.99 (2.00)	0.00 (0.00)	1.89 (1.88)	−2.27 (−2.28)

[a]Relative energies are given at 0 K in eV; the values in parentheses correspond to the relative Gibbs energies at 298 K. [b]Solvent effect is included by PCM calculations.

the *O*- and *N*-deprotonated complexes in that the latter is only 0.03 eV higher in energy than the former.

Hence, let us conclude that the *N*-deprotonated forms of the metal complexes of hydroxamates are the key intermediates in the Lossen rearrangements. The microscopic rates of the Lossen rearrangement will be similar for all complexes as implied by the similar barrier heights for this step, but the overall rate will be largest for the potassium complex, because the population of the key intermediate, that is, the metal complex of *N*-deprotonated hydroxamate, will be the largest. Simple kinetic modeling of this reaction indeed confirms this trend.

Having suggested the mechanism for the potassium catalyzed Lossen rearrangement computationally, we wanted to probe the structure of the key intermediate also experimentally. The potassium complexes are neutral and hence cannot by sampled by ESI-MS. The experiments were therefore performed with a charge-tagged molecule;[21−23] namely with benzhydroxamic acid bearing a trimethylamonium group (the charge-tag) in the *meta* position of the aromatic ring (**2**, (3-hydroxycarbamoylphenyl)-trimethylamonium cation). The introduction of the charge-tag results in a larger stabilization of the *N*-deprotonated form of the complex ($A2_{tag}$_K). It is 0.18 eV more stable than the *O*-deprotonated form ($A1_{tag}$_K) and hence we should be able to study the reactive *N*-deprotonated isomer in the gas phase.

The collision-induced dissociation of the charge-tagged complex leads either to the loss of potassium, or to the elimination of potassium hydroxide. At larger collision energies also subsequent fragmentations of the tagged phenylisocyanate are observed, namely a loss of one methyl group or methane from the trimethylamonium group and a loss of the NCO group (Figure 4). Evaluation of the collision-energy dependent CIDs for the K^+ channel and the KOH-loss channel leads to the same threshold energies (E_{thres} = 1.7 ± 0.1 eV; the energy demand is about 0.3 eV lower that predicted by the computations; see the SI).

The potential-energy surface for the Lossen rearrangement of the potassium complex of the tagged hydroxamate $[(\mathbf{2}\text{-H})K]^+$ (Figure 5) is analogous to that of [(**1**-H)K], only the energy barriers are slightly higher. Elimination of the potassium cation is possible for all structures along the reaction coordinate, but the energy demands for the complexes $A1_{tag}$_K and $A2_{tag}$_K are very large (around 3 eV). Therefore, the elimination of K^+ as well as KOH can only be observed after the Lossen rearrangement, which is consistent with the identical energy thresholds of these fragmentations in the experiment. Note that two orientations of the hydroxamate group with respect to the trimethylamonium group are possible (rotation of the hydroxamate group around the C−C bond). We show only one variant in Figure 5 and also discuss only one set of

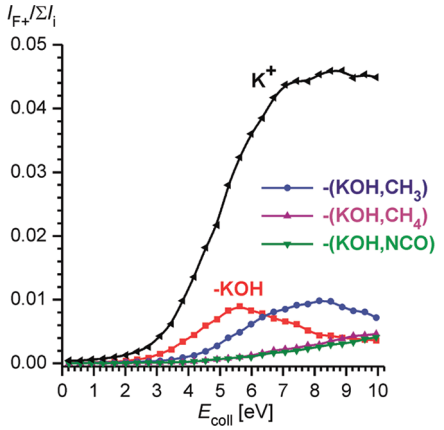

Figure 4. Energy dependent CID of $[K(2\text{-H})]^+$ (solid symbols, collision gas: Xe). For the determination of the threshold energies, see the SI.

energies; the potential-energy surface for the other conformers are analogous and can be found in the SI.

The experimental IRMPD spectrum of the charge-tagged complex $[(\mathbf{2}\text{-H})K]^+$ is shown in Figure 6a. Its comparison with the theoretical spectra clearly shows that the structure of the isolated ions corresponds to the $A2_{tag}$_K isomer (Figure 6b). Hence, we unequivocally detect the potassium complex with benzhydroxamate deprotonated at the nitrogen atom. A closer examination of the experimental spectrum reveals that a weak band at 1165 cm^{-1} does not correspond to any peak in the theoretical spectrum of $A2_{tag}$_K and can be only interpreted, if we take into account also a minor population of the less stable isomer $A1_{tag}$_K (Figure 6c). This band hence most probably corresponds to the N−O stretch of the isomer with *O*-deprotonated hydroxamate.

Under the conditions of the IRMPD experiment eliminations of K^+ and KOH are observed. The IRMPD spectra obtained, if these channels are considered separately, are almost identical (see the SI). The only difference is a band at about 1660 cm^{-1}, which can be observed only in the elimination of K^+. This band can be interpreted as the C═O stretching vibration of the carbamate product (Figure 6d). In agreement, the elimination of KOH from the carbamate product is not expected.

Finally, we have probed to which extent the conclusions from the gas-phase experiments can be transformed into the synthetic procedures. To this end, the Lossen rearrangement of *p*-methylbenzhydroxamic acid **3** was investigated. First, we have repeated the experiment reported by Hoshino et al.[8] In agreement, we have obtained quantitative yield of the product, *p*-methylaniline, after 2 h heating of *p*-methylbenzhydroxamic acid with 1 equiv of K_2CO_3 in DMF at 90 °C. The same experiment with $ZnCO_3$ did not lead to product formation.

dx.doi.org/10.1021/jo300031f | J. Org. Chem. 2012, 77, 2829−2836

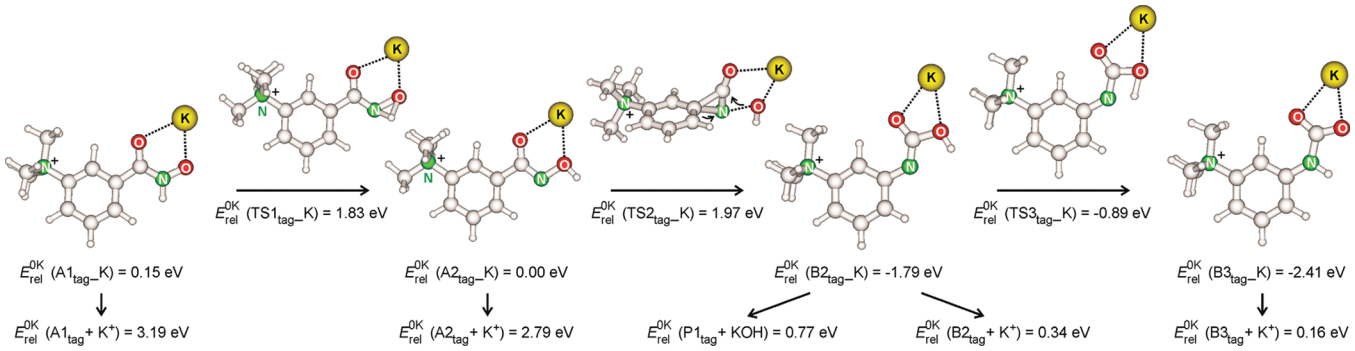

Figure 5. B3LYP/TZVP potential-energy surface for the potassium-assisted Lossen rearrangement of the charge-tagged benzhydroxamic acid. Energies refer to 0 K in the gas phase and are given relative to E^{0K}(A2$_{tag}$–K) = −1249.156315 hartree. The lowest line shows the fragmentation pathways for the eliminations of K$^+$ or KOH, respectively.

The reaction mixtures are heterogeneous; therefore it is difficult to estimate the actual concentration of the catalyst. In order to make a direct comparison, we have taken soluble metal acetates as catalysts (Table 3). These salts are less basic and therefore the deprotonation of the hydroxamic acid is slower or less efficient. Nevertheless, even though acetic acid is a stronger acid than hydroxamic acids, the transmetalation between acetate and hydroxamate occurs due to the chelating capabilities of the hydroxamic acids.[24,25] The reaction of the hydroxamic acid with potassium acetate in DMSO at 140 °C gives 57% yield after 2 h. Under the same conditions, the catalysis by zinc acetate leads only to 5% of the product and even after 8 h only 18% of the product is formed. This experiment thus clearly shows that coordination to a metal leads to the Lossen rearrangement. The small yield in the zinc-catalyzed reaction agrees well with the suggested mechanism.

To exclude mechanisms involving the formation of a carbamoylhydroxamate (Scheme 2), we have prepared the potassium hydroxamate salt in a separate step, dissolved it in water and refluxed for two hours. This procedure leads to 47% yield of the product (the remaining part was the unreacted salt). The use of water as the reaction medium prevents the formation of carbamoylhydroxamate, and therefore, the suggested metal-assisted rearrangement remains as the only possible mechanistic variant for this reaction.

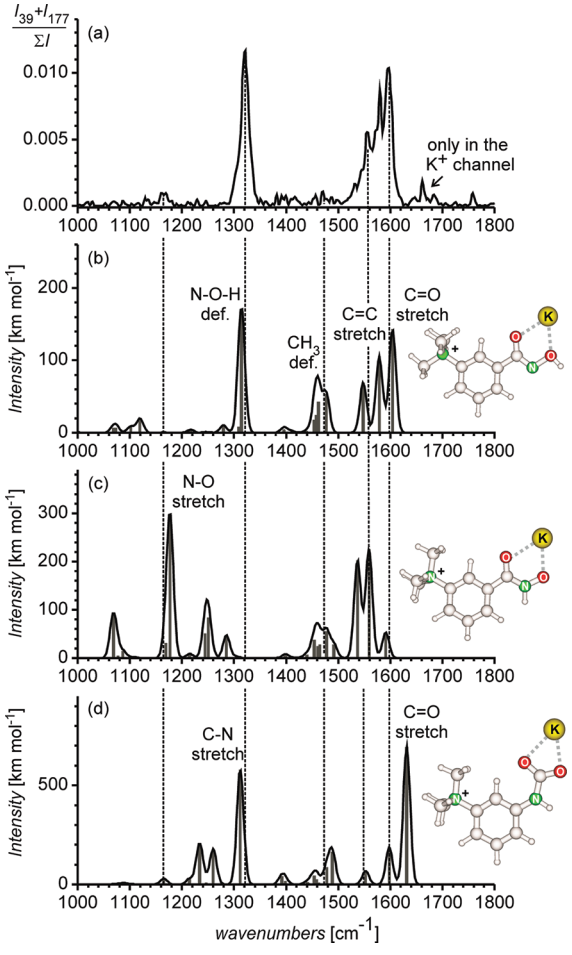

Figure 6. IRMPD spectrum of [(**2**-H)K]$^+$ (a) and its comparison with calculated IR spectra of different isomers of the complex (b-d). The theoretical spectra are shown as gray bars, the black solid lines show the theoretical spectra folded with a Gaussian function (fwhm =16 cm^{-1}). Notations I_{39}, I_{177} and ΣI refer to the relative intensities of the fragments K$^+$ (m/z 39), [(**2**-H$_2$O)]$^+$ (m/z 177) and the sum of both mentioned intensities and that of the parent ion [(**2**-H)K]$^+$ (m/z 233), respectively.

■ CONCLUSIONS

Using a combined approach of several experimental methods and theory we have demonstrated that the Lossen rearrangement can be efficiently catalyzed by metals. The reaction sequence starts with the formation of a metal complex of a deprotonated hydroxamate. The classical metal complexes are deprotonated at the oxygen atom of the hydroxamates. The Lossen rearrangement is initiated by a hydrogen migration from the nitrogen atom to the oxygen atom (Scheme 3). The nitrogen-deprotonated form of the metal hydroxamate undergoes the Lossen rearrangement to yield a metal carbamate. The last step consists in a facile hydrogen migration from oxygen to nitrogen to yield the final product.

We have characterized complexes between zinc and benzhydroxamate using IRMPD spectroscopy and proved that the hydroxamate is deprotonated at the oxygen atom, as expected. We have also characterized a complex between potassium and benzhydroxamate bearing a trimethylamonium group (charge tag) at the aromatic ring. It is unequivocally shown that in the tagged complex the hydroxamate is deprotonated at the nitrogen atom. DFT calculations show that the same situation can be expected also for the nontagged potassium benzhydroxamate, if the effect of the solvent is taken into account. The potential-energy surface for the metal-catalyzed Lossen rearrangement reveals that the reaction

dx.doi.org/10.1021/jo300031f | J. Org. Chem. 2012, 77, 2829−2836

Table 3. Lossen Rearrangement of *p*-Methylbenzhydroxamic Acid (3) under Different Conditions

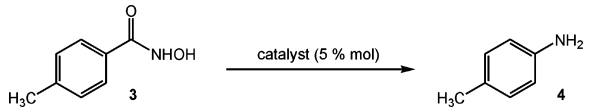

entry	catalyst	solvent	temperature (°C)	time (h)	yield[a] (%)
3	K_2CO_3	DMSO	140	2	quantitative
3	CH_3COOK	DMSO	140	2	57
3	$Zn(CH_3COO)_2$	DMSO	140	2	5
3	$Zn(CH_3COO)_2$	DMSO	140	8	18
[K(**3**-H)]		H_2O	100	2	47

[a] ^{1}H NMR yields.

Scheme 3. Mechanism of the Metal-assisted Lossen Rearrangement

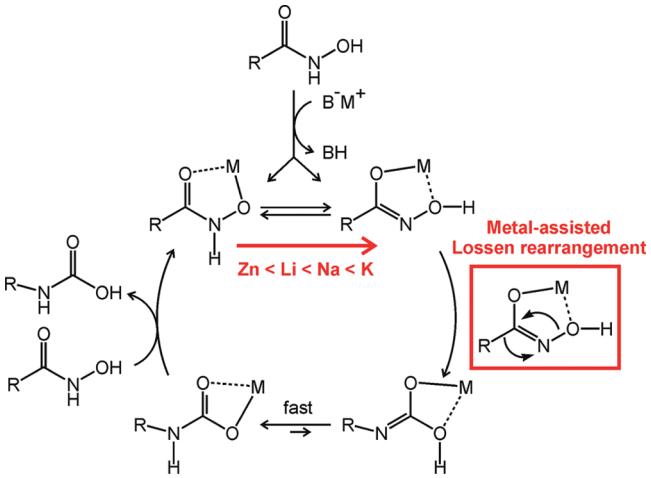

efficiency is associated mainly with relative stabilities of *O*- and *N*-deprotonated forms of the hydroxamate. For the potassium complexes, the largest ratio of the reactive *N*-deprotonated complex is expected, which correlates with largest yields of the product of the Lossen rearrangement observed experimentally.

EXPERIMENTAL AND COMPUTATIONAL DETAILS

Gas-phase infrared (IR) spectra of mass-selected ions were recorded using an ion trap mass spectrometer mounted to a free electron laser at CLIO (Centre Laser Infrarouge Orsay, France).[26] The ions were generated by electrospray ionization (ESI) of methanolic solutions of a metal salt and the hydroxamic acid of interest (for the zinc complexes phenanthroline was added as a coligand). The free electron laser (FEL) was operated at 44 MeV electron energy which provided light in a 1000−1800 cm^{-1} range. The relative spectral line width of the FEL is of about 1% and the precision of the measurement of the wavenumbers with a monochromator is about 1 cm^{-1}. The ions were mass-selected and stored in the ion trap. The fragmentation was induced by 5 to 10 laser macropulses of 8 μs admitted to the ion trap. The dependence of the fragmentation intensities on the wavelength of the IR light gives the infrared multiphoton dissociation (IRMPD) spectra. The reported IRMPD spectra are averages of 2 raw spectra. Each point in a raw spectrum at a given wavelength is obtained by the evaluation of 4 mass spectra in that each mass spectrum is an average of 5 measurements. The IRMPD spectra are not corrected for the power of the free-electron laser, which slightly changes in dependence of the wavenumbers (Figure S4 the SI).

Density functional theory calculations were performed using the B3LYP hybrid functional[27−30] together with the triple ζ basis set TZVP[31] as implemented in the Gaussian 09.[32] All minima and transition structures were verified by analysis of their Hessian matrixes. The calculated infrared spectra are scaled according to the best agreement between theory and experiment.[33] The scaling factors were 0.980 for the zinc complexes and 0.965 for the potassium complexes. For the transition structures, also intrinsic reaction coordinates were calculated at the same level of theory.[34,35] All minima and transition states were further reoptimized using the polarized continuum model for modeling the effect of solvent[36] and frequency calculations were again performed in order to control the identity of the stationary points as well as to obtain thermochemical corrections for energies at 0 K and Gibbs energies at 298 K.

All chemicals were obtained from commercial sources (including 3-(hydroxycarbamoylphenyl)trimethylamonium iodide). ^{1}H NMR spectra were recorded in a DMSO-d_6 solutions (^{1}H NMR at 300 MHz). 4-Methylbenzhydroxamic acid (**3**) was prepared according to previously reported procedures.[8] The potassium salt of 4-methylbenzhydroxamic acid ([K(**3**-H)]) was prepared by neutralization of the acid **3** with KOH in methanol. Detailed descriptions of preparation of [K(**3**-H)] and all ^{1}H NMR spectra can be found in the Supporting Information.

ASSOCIATED CONTENT

Supporting Information

Data, evaluation, and details about collision-induced dissociation experiments, IRMPD experiments and their evaluation for the $[(\mathbf{1}\text{-H})(\mathbf{1})Zn]^+$ complex, theoretical results (optimized geometries and energetics for all calculated structures) and complete ref 32. This material is available free of charge via the Internet at http://pubs.acs.org.

AUTHOR INFORMATION

Corresponding Author

*roithova@natur.cuni.cz

Notes

The authors declare no competing financial interest.

ACKNOWLEDGMENTS

We gratefully acknowledge financial support from the Grant agency of the Czech Republic (207/11/0338), the European Research Council (StG ISORI), and the Ministry of Education of the Czech Republic (MSM0021620857). Philippe Maitre and the CLIO staff, particularly Vincent Steinmetz, are gratefully acknowledged for their help and assistance.

REFERENCES

(1) Hurd, C. D.; Bauer, L. *J. Am. Chem. Soc.* **1954**, *76*, 2791.
(2) Stafford, J. A.; Gonzales, S. S.; Barrett, D. G.; Suh, E. M.; Feldman, P. L. *J. Org. Chem.* **1998**, *63*, 10040.
(3) Stolberg, M. A.; Tweit, R. C.; Steinberg, G. M.; Wagner-Jauregg, T. *J. Am. Chem. Soc.* **1955**, *77*, 765.
(4) Pihuleac, J.; Bauer, L. *Synthesis* **1989**, 61.
(5) (a) Hoare, D. G.; Olson, A.; Koshland, D. E. Jr. *J. Am. Chem. Soc.* **1968**, *90*, 1638.

(6) Narendra, N.; Chennakrishnareddy, G.; Sureshbabu, V. V. *Org. Biomol. Chem.* **2009**, *7*, 3520.
(7) Dube, P.; Nathel, N. F. F.; Vetelino, M.; Couturier, M.; Larrivee Aboussafy, C.; Pichette, S.; Jorgensen, M. L.; Hardink, M. *Org. Lett.* **2009**, *11*, 5622.
(8) Hoshino, Y.; Okuno, M.; Kawamura, E.; Honda, K.; Inoue, S. *Chem. Commun.* **2009**, 2281.
(9) Ducháčková, L.; Roithová, J. *Chem.—Eur. J.* **2009**, *15*, 13399.
(10) (a) Bauer, L.; Exner, O. *Angew. Chem., Int. Ed. Engl.* **1974**, *13*, 376. (b) Exner, O.; Hradil, M.; Mollin, J. *Collect. Czech. Chem. Commun.* **1993**, *58*, 1109. (c) Bagno, A.; Comuzzi, C.; Scorrano, G. *J. Am. Chem. Soc.* **1994**, *116*, 916. (d) Senent, M. L.; Nino, A.; Caro, C. M.; Ibeas, S.; Garcia, B.; Leal, J. M.; Secco, F.; Venturini, M. *J. Org. Chem.* **2003**, *68*, 6535.
(11) Codd, R. *Coord. Chem. Rev.* **2008**, *252*, 1387 and references therein..
(12) (a) MacAleese, L.; Maitre, P. *Mass Spectrom. Rev.* **2007**, *26*, 583 and references therein. (b) Polfer, N. C.; Oomens, J. *J. Mass Spectrom. Rev.* **2009**, *28*, 468. (c) Roithová, J. *Chem. Soc. Rev.* **2012**, *41*, 547.
(13) Ducháčková, L.; Schröder, D.; Roithová, J. *Inorg. Chem.* **2011**, *50*, 3153.
(14) Wentrup, C. *Acc. Chem. Res.* **2011**, *44*, 393 and references therein..
(15) (a) Armentrout, P. B.; Ervin, K. M.; Rodgers, M. T. *J. Chem. Phys.* **2008**, *112*, 10071. (b) Amicangelo, J. C.; Armentrout, P. B. *Int. J. Mass Spectrom.* **2011**, *301*, 45.
(16) Narancic, S.; Bach, A.; Chen, P. *J. Phys. Chem. A* **2007**, *111*, 7006.
(17) Albu, T. V.; Lynch, B. J.; Truhlar, D. G.; Goren, A. C.; Hrovat, D. A.; Borden, W. T.; Moss, R. A. *J. Phys. Chem. A* **2002**, *106*, 5323.
(18) (a) Ducháčková, L.; Steinmetz, V.; Lemaire, J.; Roithová, J. *Inorg. Chem.* **2010**, *49*, 8897. (b) Rezabel, E.; Ducháčková, L.; Milko, P.; Holthausen, M. C.; Roithová, J. *Inorg. Chem.* **2010**, *49*, 8421.
(19) Schröder, D.; Roithová, J; Gruene, P; Schwarz, H; Mayr, H; Koszinowski, K. *J. Phys. Chem. A* **2007**, *111*, 8925.
(20) Kozuch, S.; Shaik, S. *Acc. Chem. Res.* **2011**, *44*, 101.
(21) Examples of ESI-MS studies of reaction mechanisms: (a) Putau, A.; Koszinowski, K. *Organometallics* **2011**, *30*, 4771. (b) Robbins, D. W.; Hartwig, J. F. *Science* **2011**, *333*, 6048. (c) Agrawal, D.; Schröder, D.; Frech, C. M. *Organometallics* **2011**, *30*, 3579. (d) Schwarz, H. *Angew. Chem., Int. Ed.* **2011**, *50*, 10096. (e) Perry, R. H.; Splendore, M.; Chien, A.; Davis, N. K.; Zare, R. N. *Angew. Chem., Int. Ed.* **2011**, *50*, 250. (f) Coelho, F.; Eberlin, M. N. *Angew. Chem., Int. Ed.* **2011**, *50*, 5261. (g) Koszinowski, K. *J. Am. Chem. Soc.* **2010**, *132*, 6032. (h) Wassenaar, J.; Jansen, E.; van Zeist, W. J.; Bickelhaupt, F. M.; Siegler, M. A.; Spek, A. L.; Reek, J. N. H. *Nat. Chem.* **2010**, *2*, 417. (i) Roithová, J.; Milko, P. *J. Am. Chem. Soc.* **2010**, *132*, 281. (j) Schlangen, M.; Schwarz, H. *Chem. Commun.* **2010**, *46*, 1878. (k) Couzijn, E. P. A; Zocher, E.; Bach, A.; Chen., P. *Chem.—Eur. J.* **2010**, *16*, 5408. (l) Fedorov, A.; Couzijn, E. P. A; Nagornova, N. S.; Boyarkin, O. V.; Rizzo, T. R.; Chen, P. *J. Am. Chem. Soc.* **2010**, *132*, 13789. (m) Crestoni, M. E.; Fornarini, S.; Lanucara, F.; Warren, J. J.; Mayer, J. M. *J. Am. Chem. Soc.* **2010**, *132*, 4336. (n) Amarante, G. W.; Milagre, H. M. S.; Vaz, B. G.; Ferreira, B. R. V.; Eberlin, M. N.; Coelho, F. *J. Org. Chem.* **2009**, *74*, 3031. (o) Crestoni, M. E.; Fornarini, S. *Inorg. Chem.* **2005**, *44*, 5379.
(22) Review articles: (a) Eberlin, M. N. *Eur. J. Mass Spectrom.* **2007**, *13*, 19. (b) Chen, P. *Angew. Chem., Int. Ed.* **2003**, *42*, 2832.
(23) Schade, M. A.; Feckenstein, J. E.; Knochel, P.; Koszinowski, K. *J. Org. Chem.* **2010**, *75*, 6848.
(24) Vannini, A.; Volpari, C.; Filocamo, G.; Casavola, E. C.; Brunetti, M.; Renzoni, D.; Chakravarty, P.; Paolini, C.; De Francesco, R.; Gallinari, P.; Steinkuhler, C.; Di Marco, S. *Proc. Natl. Acad. Sci. U.S.A.* **2004**, *101*, 15064.
(25) Dowling, D. P.; Gantt, S. L.; Gattis, S. G.; Fierke, C. A.; Christianson, D. W. *Biochemistry* **2008**, *47*, 13554.
(26) Ortega, J. M.; Glotin, F.; Prazeres, R. *Infrared Phys. Technol.* **2006**, *49*, 133.
(27) Vosko, S. H.; Wilk, L.; Nusair, M. *Can. J. Phys.* **1980**, *58*, 1200.
(28) Lee, C.; Yang, W.; Parr, R. G. *Phys. Rev. B* **1988**, *37*, 785.
(29) Miehlich, B.; Savin, A.; Stoll, H.; Preuss, H. *Chem. Phys. Lett.* **1989**, *157*, 200.
(30) Becke, A. D. *J. Chem. Phys.* **1993**, *98*, 5648.
(31) Schaefer, A.; Huber, C.; Ahlrichs, R. *J. Chem. Phys.* **1994**, *100*, 5829.
(32) Frisch, M. J. et al. *Gaussian 09*, Revision A.02; Gaussian, Inc.: Wallingford, CT, 2009.
(33) For the method B3LYP/6-311+G(d,p) (the basis set is closest to our selection from those that have been systematically studied) a scaling factor of 0.9688 is suggested in work: Merrick, J. P.; Moran, D.; Radom, L. *J. Phys. Chem. A* **2007**, *111*, 11683 . This scaling, however, does not lead to an agreement with the experimental spectra..
(34) Gonzalez, C.; Schlegel, H. B. *J. Chem. Phys.* **1989**, *90*, 2154.
(35) Gonzalez, C.; Schlegel, H. B. *J. Phys. Chem.* **1990**, *94*, 5523.
(36) Tomasi, J.; Mennucci, B.; Cammi, R. *Chem. Rev.* **2005**, *105*, 2999.